

Autonomous Vehicle Controllers From End-to-End Differentiable Simulation

Asen Nachkov¹ Danda Pani Paudel¹ Luc Van Gool^{1,2}

¹INSAIT, Sofia University
Sofia, Bulgaria

²ETH Zurich
Zurich, Switzerland

Abstract—Current methods to learn controllers for autonomous vehicles (AVs) focus on behavioural cloning. Being trained only on exact historic data, the resulting agents often generalize poorly to novel scenarios. Simulators provide the opportunity to go beyond offline datasets, but they are still treated as complicated black boxes, only used to update the global simulation state. As a result, these RL algorithms are slow, sample-inefficient, and prior-agnostic. In this work, we leverage a differentiable simulator and design an analytic policy gradients (APG) approach to training AV controllers on the large-scale Waymo Open Motion Dataset. Our proposed framework brings the differentiable simulator into an end-to-end training loop, where gradients of the environment dynamics serve as a useful prior to help the agent learn a more grounded policy. We combine this setup with a recurrent architecture that can efficiently propagate temporal information across long simulated trajectories. This APG method allows us to learn robust, accurate, and fast policies, while only requiring widely-available expert trajectories, instead of scarce expert actions. We compare to behavioural cloning and find significant improvements in performance and robustness to noise in the dynamics, as well as overall more intuitive human-like handling.

I. INTRODUCTION

When training AV controllers, it is common to treat the environment as a black-box function that is only used to evolve the states and provide an interactive element to the data collection process. Different RL algorithms adopt different strategies for handling it.

By using replay buffers to store past transitions, value-based [20], model-based [30], or policy gradient [32] methods are oblivious to how the next state has been generated. They treat it as either a target or some state from which to bootstrap a value estimate. This approach is general, but makes training slow and sample-inefficient, since the world dynamics and a behavioural policy have to be learned from the data. Imitation learning [5], being essentially supervised learning on expert actions, is more sample-efficient but suffers from generalization difficulties and avoids learning virtually any kind of dynamics information.

If the environment dynamics are known one would likely be able to harvest the best aspects from each of these methods. In fact, in a differentiable environment one can optimize the policy directly using gradient descent, just via supervision from expert agent trajectories, as shown in Fig. 1. The benefits of this are: 1) Obtaining an *explicit policy for continuous control*, 2) *Fast inference*, since there is no

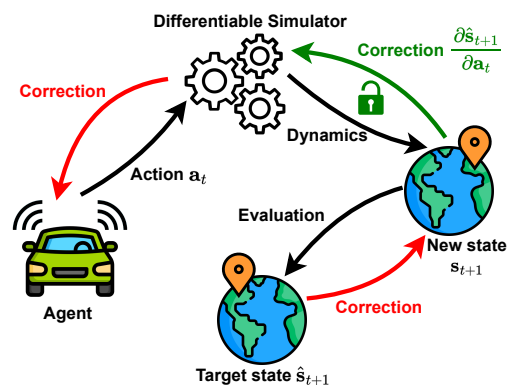


Fig. 1: **End-to-end learning of controllers.** Our framework utilizes a differentiable simulator to learn autonomous vehicle controllers from the corrections between the simulated new states and the target states.

planning at test time, 3) *Unbounded policy precision*, due to the dynamics not being approximated, 4) Facilitating more *grounded learning* by incorporating the dynamics directly into the training loop. This occurs by computing gradients of the dynamics, along with the usual derivatives, within the backpropagation, and using them to update the policy.

Waymax [10] was recently introduced as a differentiable, large-scale autonomous driving simulator. In this work, we utilize its differentiability to train controllers using Analytic Policy Gradients (APG), reaping all the benefits mentioned above. We cleverly design our model to not require differentiating through the simulator state, only through the dynamics. Combining this with a recurrent architecture that propagates temporal information across long simulated trajectories allows us to flow the dynamics gradients to earlier steps (trace the blue arrows in Fig. 3), improving training speed and performance. To the best of our knowledge, we are the first to apply APG on such a large-scale task, obtaining strong competitive performance comparable to larger heavily-engineered models which do not make use of simulators.

Contributions. Our main contributions are:

- 1) We identify and utilize a set of gradients obtainable within the Waymax simulator required for the downstream task of learning AV controllers, explained in Sec. III-A In this process, we modify some operations

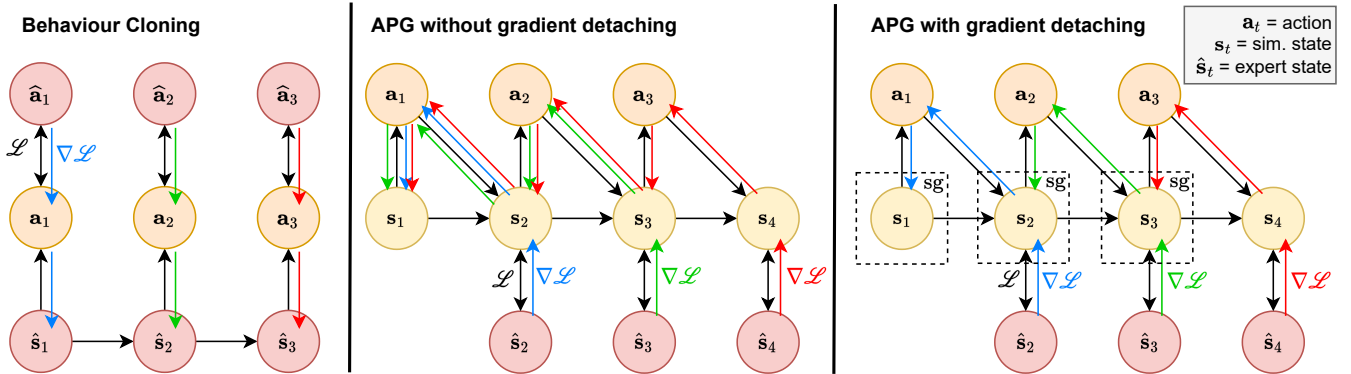


Fig. 2: **Learning with and without simulator.** Left: learning by behaviour cloning where we replay the GT trajectory and supervise the predicted actions. Middle: APG where we roll-out and supervise the trajectories without detaching gradients (shown in colored arrows). Right: APG where we detach gradients from past timesteps. The slanted arrows from \mathbf{a}_t to \mathbf{s}_{t+1} are the environment dynamics. The proposed detachment during simulation offers efficient and lightweight training.

- in the dynamics to make them gradient-friendly.
- 2) We develop a framework for end-to-end training of AV controllers using differentiable simulation and discuss its particular design implications and model constraints in Section III-B and III-C.
- 3) We train and evaluate a model based on APG, in Sec. IV, which attains strong performance while being more accurate and more robust than relevant baselines.

II. RELATED WORK

RL methods that consider the environment as a black box, have different ways to learn a policy without the gradients of the dynamics, as shown in Table I. Because of that, most of them do not incorporate any world priors that are otherwise contained in the simulator. Compared to them, the analytic policy gradients approach (APG) is stable, sample efficient, and fast at test time. It has been used for trajectory tracking in drones [36], and is increasingly being used in differentiable physics simulators for robotics [8], [9], [12], [22], [18].

Method	Pros	Cons
Value-learning [20], [2], [35], [33]	Stable, guaranteed convergence	Implicit policy, moving target optimization
Policy gradients [32], [17], [27], [28]	Intuitive, scales well	Unstable, sample-inefficient, converges to local optima
Model-based [30], [26], [39]	Offline, planning	Slow, bounded by precision of dynamics model
Imitation learning [5], [16]	Scales well, offline	Non robust, generalization difficulty [6]

TABLE I: **Different controller-training methods.** All of them consider the environment as a black box.

Relevance to BPTT. APG is similar to backpropagation-through-time (BPTT) in that both typically differentiate the forward pass of a system component through multiple

timesteps. In the case of RNNs [11], [1] it is the application of a recurrent cell that is differentiated multiple times, whereas with APG it is the dynamics of an environment [23]. Since in traditional sequence modeling (e.g. machine translation [31]) the observed feature sequences do not depend on the recurrent model outputs, a better comparison to APG is optimizing recurrent policy networks [37], [25]. In such cases vanishing or exploding gradients have been observed, stemming from the spectrum of the Jacobian of the environment dynamics [19].

Modern approaches to trajectory prediction. Recently, trajectory prediction for AVs has been dominated by transformer models [29], [38], [24], [13]. Specifically, MTR [29] uses a transformer encoder to predict an initial per-agent trajectory and collect map features alongside it. It then refines this trajectory using a transformer decoder. MVTA [34] adapts MTR for closed-loop simulation, as required by WOSAC [21], by introducing receding-horizon predictions and variable-length history aggregation. Other models focus on collision-avoidance [4] or interactivity between agents in order to improve performance [15]. All these methods directly predict future locations, not actions, and therefore do not rely on any simulations.

III. METHOD

In essence, a differentiable environment allows us to backpropagate gradients through it and directly optimize the policy. The resulting method broadly falls into the *analytic policy gradients* (APG) type of algorithms. In our setting we assume we are given expert trajectories $\{\hat{\mathbf{s}}_t\}_{t=1}^T$, instead of rewards. The goal is to train the policy π_θ so that upon a roll-out, it reproduces the expert trajectory:

$$\min_{\theta} \mathcal{L} = \frac{1}{T} \sum_{t=1}^T \|\hat{\mathbf{s}}_t - \mathbf{s}_t\|_2, \quad (1)$$

where $\mathbf{s}_t = \text{Env}(\mathbf{s}_{t-1}, \mathbf{a}_{t-1})$ and $\mathbf{a}_{t-1} \sim \pi_\theta(\mathbf{s}_{t-1})$

Here $\hat{\mathbf{s}}_t$ and $\hat{\mathbf{a}}_t$ refer to ground truth states and actions while \mathbf{s}_t and \mathbf{a}_t are the corresponding simulated states and actions. The sequence of states $\{\mathbf{s}_t\}_{t=1}^T$ forms a trajectory.

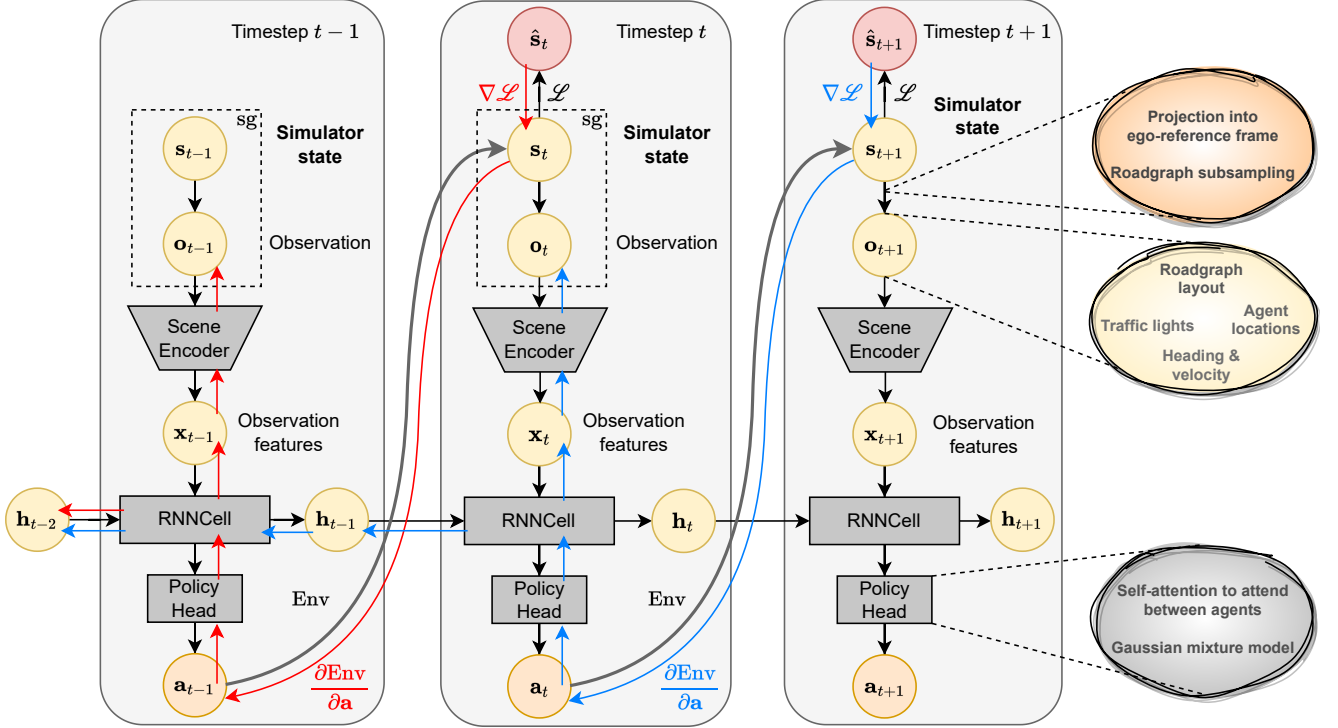


Fig. 3: **Unrolling the model in time with gradient detachment inside the differentiable simulator.** Starting from the simulator state \mathbf{s}_t , we obtain an observation \mathbf{o}_t , containing the scene elements such as agents locations, traffic lights, and roadgraph, which gets encoded into features \mathbf{x}_t . An RNN (recurrent over time) with a policy head outputs actions \mathbf{a}_t which are executed in the simulated environment to obtain the new state \mathbf{s}_{t+1} . When applying a loss between \mathbf{s}_{t+1} and $\hat{\mathbf{s}}_{t+1}$ the gradients flow back through the environment and update the policy head, RNN, and the scene encoder. Similar to BPTT, gradients through the RNN hidden state accumulate. We do not backpropagate through the observation or the simulator state.

Optimization task (1) is difficult because trajectories are generated in a sequential manner with current states depending on previous actions, which themselves recursively depend on previous states. Additionally, $\nabla_{\theta} \mathcal{L}$ (we show for only one of its additive terms) has the form

$$\frac{\partial \mathcal{L}}{\partial \theta} = \frac{\partial \mathcal{L}}{\partial \mathbf{s}_t} \frac{\partial \mathbf{s}_t}{\partial \mathbf{a}_{t-1}} \frac{\partial \mathbf{a}_{t-1}}{\partial \mathbf{s}_{t-1}} \frac{\partial \mathbf{s}_{t-1}}{\partial \mathbf{a}_{t-2}} \cdots \frac{\partial \mathbf{a}_0}{\partial \theta} \quad (2)$$

which multiplicatively composes multiple derivatives $\frac{\partial \mathbf{s}_t}{\partial \mathbf{a}_{t-1}}$ corresponding to the environment dynamics themselves. Depending on the spectrum of the dynamics, these gradients may vanish or explode.

Application setting. Ultimately, for motion perception and planning in autonomous vehicles, we are interested in multi-modal trajectory prediction. Given a short history segment for all agents in the scene, we want to obtain K modes, or possible trajectories, for the future of each agent. In the presence of a simulator we can learn a stochastic policy, or controller, for the agents. Then, we can perform K roll-outs, obtaining K future trajectories. Hence, in the presence of a simulator, the task of trajectory prediction reduces to learning a policy $\pi_{\theta} : \mathbf{s}_t \mapsto \mathbf{a}_t$ to control the agents.

A. Differentiating through Waymax

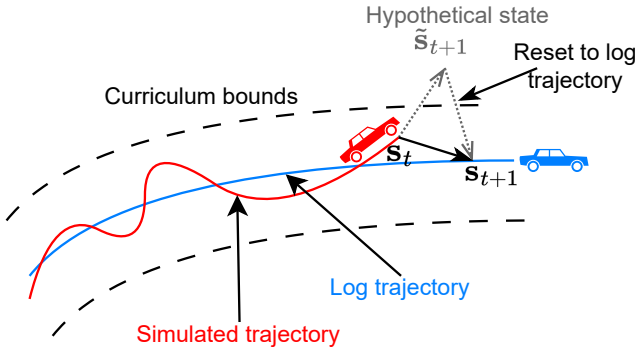
Obtaining gradients. We apply our APG method in the Waymax simulator [10]. Being implemented in Jax [3], it is

relatively flexible in choosing which variable to differentiate and with respect to what. That being said, many of the *obtainable* derivatives are not meaningful. For example,

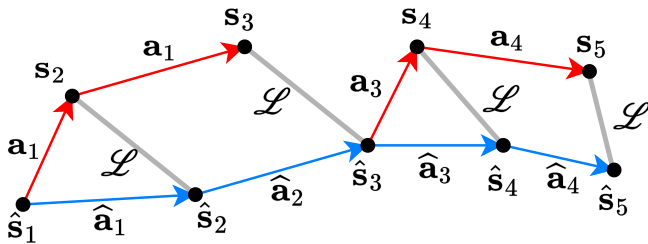
- 1) The derivatives of future agent locations with respect to current traffic light states or roadgraphs are all zero, because the simulator dynamics (e.g., bicycle or delta dynamics) do not depend on the roadgraph or the traffic lights. There are no rigid-body collisions.
- 2) Certain metrics such as collision or offroad detection are boolean in nature. Other objects such as traffic lights have discrete states. While useful for training, these are problematic for differentiation.

What is *meaningful* and *useful* is to take the gradients of future controllable agent locations with respect to their current actions, $\partial \mathbf{s}_t / \partial \mathbf{a}_{t-1}$. These are precisely the derivatives needed for objective (1) and hence we focus on them. We treat the dynamics as another function in the computation graph, while ensuring that the relevant code structures for training are registered in Jax's `pytree` registry, so that any tracing, just-in-time compilation, or functional transformations like `grad` can be applied on them.

Moreover, we found it useful to adapt the bicycle dynamics model to be gradient-friendly. This includes adding a small epsilon to the argument of a square root to avoid the case when its input is 0, as well as adapting the yaw angle wrapping, present in many similar settings, to use `arctan2`



(a) Resetting based on distance.



(b) Resetting based on time.

Fig. 4: **Resetting agent’s state during incremental learning.** We can do so either (a), based on distance, whenever the agent goes too far from the log trajectory, or (b) every few timesteps. A loss (shown in grey) is computed on all timesteps, but the collected trajectory (red) is discontinuous.

instead of `mod`, which makes the corresponding derivatives continuous and facilitates training.

B. End-to-end training with the simulator

Dense trajectory supervision. Obtaining the gradients of the environment dynamics opens up technical questions of how to train in such a setup. One can supervise the rolled-out trajectory only at the final state and let the gradients flow all the way back to the initial state. Since this does not supervise the *path* taken to the objective, in our experiments we densely supervise all states in the collected trajectory with all states in the GT trajectory.

Gradient detaching. Dense supervision allows us to detach the gradients at the right places, as shown in the third part of Fig. 2. Here, when we obtain s_t , we calculate the loss and backpropagate through the environment dynamics obtaining $\partial s_t / \partial \mathbf{a}_{t-1}$ without continuing on to previous steps. This makes training slower, since gradients for the earlier steps do not accumulate, as in a RNN, but effectively cuts the whole trajectory into many $(s_t, \mathbf{a}_t, s_{t+1})$ transitions which can be treated independently by the optimization step. This allows for *off-policy* training – a key aspect of our setup.

C. Model overview

We present our model setup in Figure 3. For training, we roll-out a full trajectory and supervise with the GT one. The gradients flow back through the differentiable dynamics, policy and scene encoder, and continue back to the previous scene contexts using a RNN hidden state. We detach the previous simulator state for both *necessity* and *flexibility* so

that the state transitions on which we compute the loss can be different from the transitions executed during roll-out.

Optimization difficulty. Differentiating through a stochastic policy requires that the actions be reparametrized [14]. But every reparametrization leads to stochastic gradients for those layers before it. And when we compose sampling operations sequentially, such as in the computation graph of the entire collected trajectory, the noise starts to compound and may overwhelm the actual signal from the trajectory steps, making the optimization more noisy and difficult. To address this, we implement *incremental* training where we periodically “reset” the simulated state back to the corresponding log state [36], shown in Fig. 4. This ensures that the data-collection stays around the GT trajectory, instead of far from it, increasing sample efficiency. For incremental learning, we increase the difficulty by reducing the reset frequency as training progresses.

Agent processing. For the multi-agent experiments described in Sec. IV-A we slightly adapt our architecture to allow training with N agents but evaluating with M . We adopt a small transformer that forces each agent to attend to the other ones in parallel. However, at the last transformer block we use a fixed number of learned queries which attend over the variable number of agent keys and values, effectively soft-clustering them, and becoming independent of their number. This allows us to train with 32 agents but evaluate with 128, as required by [7].

IV. EXPERIMENTS

An early example. To demonstrate the characteristics of APG, we first compare APG and behaviour cloning (BC) on a toy task – purposefully overfitting a single trajectory for a single agent. We are given a full-length ground-truth (GT) trajectory from the WOM dataset [7], $\{\hat{s}_t\}_{t=1}^T \in \mathbb{R}^{T \times 2}$, and are learning a controller π_θ of the form $\pi_\theta : (s_t, t) \mapsto \mathbf{a}_t$.

Behaviour cloning baseline. Since expert actions are available only on the GT trajectory, behaviour cloning replays it and is reduced to supervised learning on them: $\min_\theta \frac{1}{T} \sum_{t=1}^T \|\hat{\mathbf{a}}_t - \mathbf{a}_t\|_2$, where $\mathbf{a}_t = \pi_\theta(\hat{s}_{t-1})$. In that setup at test time, when we perform a roll-out, behaviour cloning suffers from error-compounding and is unable to reproduce the GT trajectory, even though it has learned the on-trajectory actions very accurately. Very small imprecisions in the actions start to accumulate, as shown in the left part of Fig. 5.

APG. If we have access to a simulator we can perform roll-outs at train time and supervise the resulting trajectories $\{s_t\}_{t=1}^T$ with $\{\hat{s}_t\}_{t=1}^T$. This is sufficient to make the controller robust and allows it to reproduce the trajectory at test time on its own. If the policy is stochastic, the learning process becomes less sample-efficient because it becomes exponentially less likely that in a far away t , a given location (x, y) is reached. Thus, as shown in Figure 5 converging to the GT trajectory does not happen uniformly from all directions, but rather sequentially. To improve sample-efficiency, as a form of *curriculum*, we snap back the simulated trajectory whenever it goes beyond a threshold ξ with respect to $\{\hat{s}_t\}_{t=1}^T$, as in Fig 4a. Since resetting the simulated trajectory

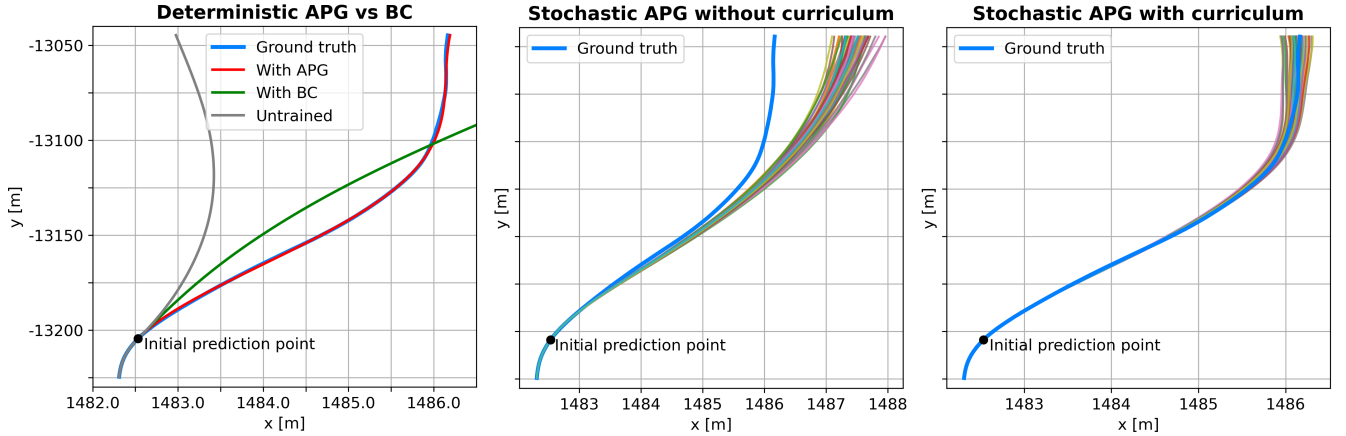


Fig. 5: **Initial results on a toy task.** x and y axes represent spatial coordinates. Left: deterministic cloning fails to reproduce the trajectory on which it was fitted, while APG succeeds. Middle: APG struggles with a stochastic policy because of the sequential nature of the task. Right: APG with periodical resetting while training improves sample efficiency.

Method	Task	Dynamics	IDM	Supervise	min ADE ↓	min overlap ↓	min offroad ↓
Rand. action	Plan	Delta	–	–	16.3925	0.5292	0.4989
Const. velocity	Plan	Delta	–	–	5.9547	0.3172	0.1150
Beh. cloning	Plan	Bicycle	✗	Actions	1.4157	0.2475	0.2673
Beh. cloning	Plan	Bicycle	✓	Actions	1.4868	0.2647	0.2132
Beh. cloning	Plan	Delta	✗	Actions	3.0063	0.1741	0.0278
Beh. cloning	Plan	Delta	✓	Actions	3.2456	0.1910	0.0330
APG, stoc.	Plan	Bicycle	✗	States	2.0083	0.0800	0.0282
APG, stoc.	Plan	Bicycle	✓	States	6.0201	0.2710	0.0560
APG, stoc.	Plan	Delta	✗	States	2.0793	0.0870	0.0200
APG, stoc.	Plan	Delta	✓	States	3.7624	0.2120	0.0370
Wayformer	Plan	Delta	✓	States	2.3800	0.1068	0.0789
Beh. cloning	Plan	Delta	✓	Actions	6.2800	0.0583	0.0414
Beh. cloning	Plan	Bicycle	✓	Actions	3.6000	0.1120	0.1359
Beh. cloning	Plan	Bicycle*	✓	Actions	2.2600	0.0459	0.0110
Beh. cloning	Plan	Delta*	✓	Actions	2.9800	0.0597	0.0442
DQN	Plan	Bicycle*	✓	Rewards	9.8300	0.0650	0.0374
DQN	Plan	Bicycle*	✓	Rewards	10.7400	0.0491	0.0431
Rand. action	Multi-agent	Bicycle	–	–	29.3291	0.8276	0.8531
Const. velocity	Multi-agent	Bicycle	–	–	9.2058	0.6997	0.7105
Beh. cloning	Multi-agent	Bicycle	–	Actions	4.1123	0.8527	0.9990
APG	Multi-agent	Bicycle	–	States	1.8096	0.6021	0.9887
Beh. cloning	Multi-agent †	Bicycle	–	Actions	9.6331	0.7587	0.9508
APG	Multi-agent †	Bicycle	–	States	3.7169	0.3953	0.5851

TABLE II: **Experimental results.** We evaluate APG and other baselines on the WOMD val set. The results in the middle block are taken from [10] as a comparable reference and all include route conditioning. * refers to the discrete version of the action space. Behavioural cloning and APG for planning have been evaluated with 32 modes. † refers to evaluating only on those objects for which `is_modeled` is set by the WOM dataset.

Method	Task	Dynamics	IDM	Supervise	min ADE ↓	min overlap ↓	min offroad ↓
APG, stoc.	Plan	Delta	✗	(x, y)	2.0806	0.5671	0.3634
APG, stoc.	Plan	Delta	✓	(x, y)	2.9700	0.5350	0.3863
APG, stoc.	Plan	Delta	✗	(x, y, v_x, v_y, θ)	2.0473	0.0880	0.0200
APG, stoc.	Plan	Delta	✓	(x, y, v_x, v_y, θ)	3.7624	0.2120	0.0376

TABLE III: **Ablation on supervising the velocity and yaw angle.** The ADE is evaluated only on (x, y) locations. We found that if we supervise not only these locations, but also the velocity and yaw angle of the agents, results are better, particularly in terms of reduced collision and offroad rates.

Method	ADE ↓	overlap ↓	overlap perc. ↓	offroad ↓	offroad perc. ↓
BC-MA	4.1123	0.8527	0.0590	0.9990	0.3657
APG-MA	1.8096	0.6021	0.0319	0.9887	0.2983
BC-MA †	9.6331	0.7587	0.0932	0.9508	0.3657
APG-MA †	3.7169	0.3953	0.0364	0.5851	0.2983

TABLE IV: **Detailed metrics for multi-agent settings.** We compare beh. cloning and APG on multi-agent simulation with bicycle dynamics. †refers to evaluating only on those objects for which `is_modeled` is set by the WOM dataset. In the perc. columns we compute the metric by averaging over all individual agent transitions, not over entire agent trajectories.

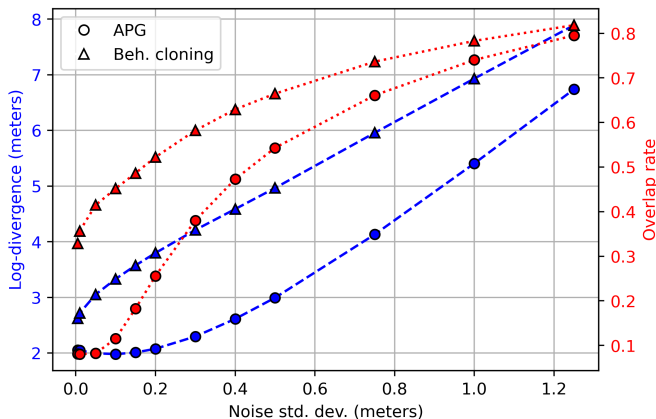


Fig. 6: **Performance comparison in a stochastic environment.** Compared to BC, the performance of APG under increasingly noisy dynamics deteriorates later. For simplicity, we do not show the offroad rates, which are similar to the overlap ones for both APG and BC.

to the GT one breaks the computation graphs, we detach the gradients as shown previously in Fig. 2.

Thus, in the extreme case when there are no additional regressors such as the roadgraph, or past agent locations, behaviour cloning fails in reproducing a GT trajectory on its own while APG does not.

A. Large-scale experiments in Waymax

Experiment setup. The Waymax simulator uses the underlying Waymo Open Motion Dataset (WOMD) [7] to initialize the simulator state. It contains close to 500K training scenarios, each of length 9 seconds and a framerate of 10 Hz. The history length is 10 frames (1 second) and the goal is to predict the next 80 frames. To train the model, we run multiple simulations, one per scenario, in parallel (this being the simulated *minibatch*) and use Adam to optimize them. We iterate through all scenarios (the equivalent of an *epoch*) multiple times. At test time, we simulate multiple roll-outs and compute the average displacement error (ADE), offroad rate, and collision rate for each mode. A collision rate of 20% means that 20% of all trajectories have *some* objects colliding at some timestep in them. Since the future is uncertain and we want to make sure that the GT locations are covered by at least one of our modes, we report the eval metrics from the best mode. Thus, we evaluate on minADE, min offroad rate, and min collision rate.

Results. Our main results are shown in Table II. We compare behavioural cloning (BC) with APG on two tasks

– *planning*, where we learn a controller only for the self-driving car, and *multi-agent* (MA), where we learn a single controller for all agents. For the latter setting, we project the roadgraph and agent coordinates in each agent’s own coordinate frame. Hence, our model is *agent-centric*. Agents’ actions are selected independently, where each agent considers the location of all others. Multi-agency results from all of them being *controlled* by the policy.

Training and evaluation specifics. For the planning task we evaluate with and without IDM [10], which makes other agents reactive to the ego-vehicle, instead of simply following the log trajectories. For MA-BC the training loss is applied over all simulated agents which have a valid GT action. For MA-APG it is applied over all agent transitions for which both the current sim agent and log agent are considered valid by the simulator. The general principle is that we must supervise the transitions of all agents controlled by the policy. We evaluate MA in two settings – on all valid objects, and on all objects for which `is_modeled` is set, according to WOMD [21].

In general, our method, outperforms those based on behavioural cloning (BC), in most cases obtaining better ADE, collision and offroad rates. It is also more certain in terms of which actions to take, leading to lower variability between individual trajectory modes. Fig. 7 shows that for our APG method, the log-divergence and overlap rates are almost independent of the number of modes. BC displays an obvious dependence and requires many modes in order for one of them to be accurate. And while with multiple modes it

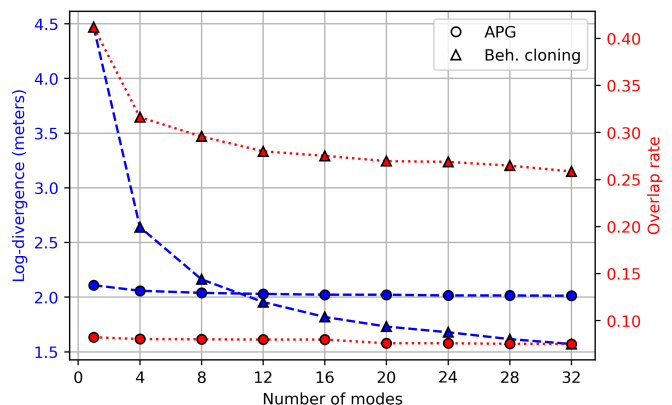


Fig. 7: **Effect of the number of modes.** Compared to BC (triangles), APG (circles) is more confident and the performance is less dependent on the number of modes.

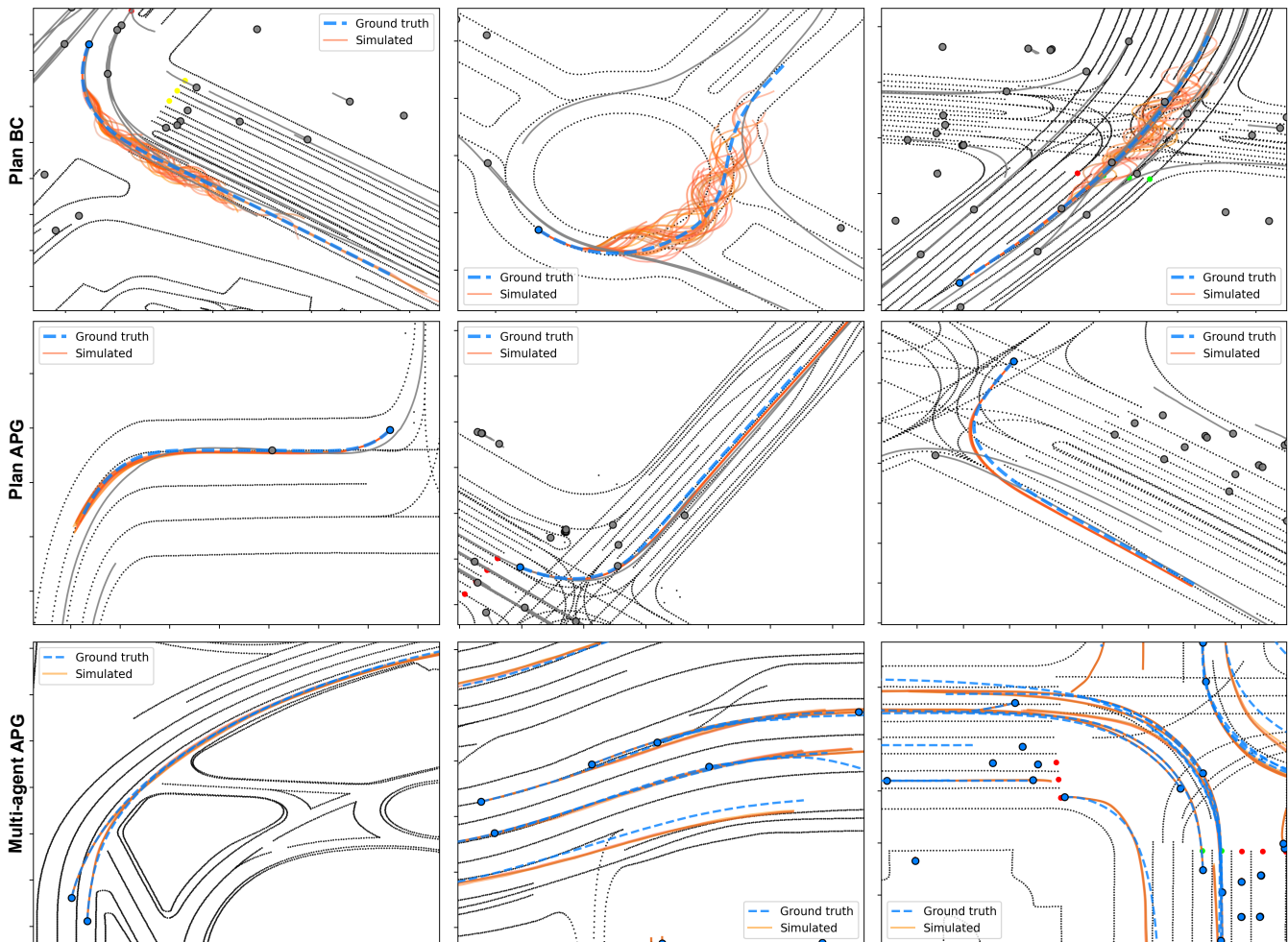


Fig. 8: **Sample trajectories.** Row 1 shows BC, while row 2 and 3 show APG applied in the planning and multi-agent control. BC produces agents that swerve, while the APG trajectories are more realistic. Blue circles show controlled agents in the beginning of the trajectory. Red, green, and yellow circles represent traffic lights.

produces lower log-divergence for the planning task, the overlap rates are still considerably worse, indicating that the trajectory is not expert-like. These results suggest that APG tends to produce more confident trajectories, which in turn allows us to save on computation, as we need to evaluate fewer modes to get a sense of the mean predicted future.

Supervision of yaw angle and velocity. Even though the log divergence metric only considers (x, y) coordinates, we supervise also with the yaw and x -, y - velocities. Table III shows that this is very beneficial for performance.

Robustness to noise and trajectory length. We perform an ablation where we make the environment dynamics stochastic at test time by adding different levels of noise to the next agent locations. Fig. 6 shows that our APG method compares favourably to BC. For very small noise levels the performance is not affected at all. Additionally, in Table V we show that training on half of each sequence, instead of the full one, reduces performance only marginally.

Qualitative study. We showcase samples from our method in Fig. 8 and observe that in the planning setting APG realizes accurate stochastic trajectories. Errors occur mostly from not predicting the correct acceleration, not the steering,

APG, plan	ADE ↓	overlap ↓	offroad ↓
Full trajectory	2.0083	0.0800	0.0282
Half trajectory	2.0493	0.0882	0.0256

TABLE V: **Shorter training sequences.** The performance is robust even when training on half the sequence lengths.

which is prevalent in the BC models and causes the agent there to swerve. The MA-APG trajectories are relatively less accurate because, unlike in planning, when all agents are controlled, any prediction will have an effect on any agent, making training more difficult.

V. CONCLUSION

In this work, we leveraged the differentiable nature of Waymax to train AV policies for planning and multi-agent control. We proposed measures – incremental learning, and a specific architecture based on an RNN for the temporal information transfer, and a transformer, for the spatial mixing of agent features – to efficiently train long episodes in diverse settings. Results suggest that our model is accurate and robust, while at the same time being lightweight and fast at inference time.

REFERENCES

- [1] Dzmitry Bahdanau, Kyunghyun Cho, and Yoshua Bengio. Neural machine translation by jointly learning to align and translate. *arXiv preprint arXiv:1409.0473*, 2014.
- [2] Marc G Bellemare, Will Dabney, and Rémi Munos. A distributional perspective on reinforcement learning. In *International conference on machine learning*, pages 449–458. PMLR, 2017.
- [3] James Bradbury, Roy Frostig, Peter Hawkins, Matthew James Johnson, Chris Leary, Dougal Maclaurin, George Necula, Adam Paszke, Jake VanderPlas, Skye Wanderman-Milne, and Qiao Zhang. JAX: composable transformations of Python+NumPy programs, 2018.
- [4] Hsu-kuang Chiu and Stephen F Smith. Collision avoidance detour for multi-agent trajectory forecasting. *arXiv preprint arXiv:2306.11638*, 2023.
- [5] Felipe Codevilla, Matthias Müller, Antonio López, Vladlen Koltun, and Alexey Dosovitskiy. End-to-end driving via conditional imitation learning. In *2018 IEEE international conference on robotics and automation (ICRA)*, pages 4693–4700. IEEE, 2018.
- [6] Felipe Codevilla, Eder Santana, Antonio M López, and Adrien Gaidon. Exploring the limitations of behavior cloning for autonomous driving. In *Proceedings of the IEEE/CVF international conference on computer vision*, pages 9329–9338, 2019.
- [7] Scott Ettinger, Shuyang Cheng, Benjamin Caine, Chenxi Liu, Hang Zhao, Sabeek Pradhan, Yuning Chai, Ben Sapp, Charles R Qi, Yin Zhou, et al. Large scale interactive motion forecasting for autonomous driving: The waymo open motion dataset. In *Proceedings of the IEEE/CVF International Conference on Computer Vision*, pages 9710–9719, 2021.
- [8] C Daniel Freeman, Erik Frey, Anton Raichuk, Sertan Girgin, Igor Mordatch, and Olivier Bachem. Brax—a differentiable physics engine for large scale rigid body simulation. *arXiv preprint arXiv:2106.13281*, 2021.
- [9] Sean Gillen and Katie Byl. Leveraging reward gradients for reinforcement learning in differentiable physics simulations. *arXiv preprint arXiv:2203.02857*, 2022.
- [10] Cole Gulino, Justin Fu, Wenjie Luo, George Tucker, Eli Bronstein, Yiren Lu, Jean Harb, Xinlei Pan, Yan Wang, Xiangyu Chen, et al. Waymax: An accelerated, data-driven simulator for large-scale autonomous driving research. *Advances in Neural Information Processing Systems*, 36, 2024.
- [11] Sepp Hochreiter and Jürgen Schmidhuber. Long short-term memory. *Neural computation*, 9(8):1735–1780, 1997.
- [12] Philipp Holl, Vladlen Koltun, and Nils Thurey. Learning to control pdes with differentiable physics. *arXiv preprint arXiv:2001.07457*, 2020.
- [13] Yihan Hu, Jiazhi Yang, Li Chen, Keyu Li, Chonghao Sima, Xizhou Zhu, Siqi Chai, Senyao Du, Tianwei Lin, Wenhai Wang, et al. Planning-oriented autonomous driving. In *Proceedings of the IEEE/CVF Conference on Computer Vision and Pattern Recognition*, pages 17853–17862, 2023.
- [14] Diederik P Kingma and Max Welling. Auto-encoding variational bayes. *arXiv preprint arXiv:1312.6114*, 2013.
- [15] Stepan Konev. Mpa: Multipath++ based architecture for motion prediction, 2022.
- [16] Luc Le Mero, Dewei Yi, Mehrdad Dianati, and Alexandros Mouzakis. A survey on imitation learning techniques for end-to-end autonomous vehicles. *IEEE Transactions on Intelligent Transportation Systems*, 23(9):14128–14147, 2022.
- [17] Sergey Levine, Chelsea Finn, Trevor Darrell, and Pieter Abbeel. End-to-end training of deep visuomotor policies. *Journal of Machine Learning Research*, 17(39):1–40, 2016.
- [18] Fanxing Li, Fangyu Sun, and Danping Zou. Visfly: An efficient and versatile simulator for training vision-based flight. *arXiv preprint arXiv:2407.14783*, 2024.
- [19] Luke Metz, C Daniel Freeman, Samuel S Schoenholz, and Tal Kachman. Gradients are not all you need. *arXiv preprint arXiv:2111.05803*, 2021.
- [20] Volodymyr Mnih, Koray Kavukcuoglu, David Silver, Andrei A Rusu, Joel Veness, Marc G Bellemare, Alex Graves, Martin Riedmiller, Andreas K Fidjeland, Georg Ostrovski, et al. Human-level control through deep reinforcement learning. *nature*, 518(7540):529–533, 2015.
- [21] Nico Montali, John Lambert, Paul Mougin, Alex Kuefler, Nicholas Rhinehart, Michelle Li, Cole Gulino, Tristan Emrich, Zoey Yang, Shimon Whiteson, et al. The waymo open sim agents challenge. *Advances in Neural Information Processing Systems*, 36, 2024.
- [22] Miguel Angel Zamora Mora, Momchil Peychev, Sehoon Ha, Martin Vechev, and Stelian Coros. Pods: Policy optimization via differentiable simulation. In *International Conference on Machine Learning*, pages 7805–7817. PMLR, 2021.
- [23] J Krishna Murthy, Miles Macklin, Florian Golemo, Vikram Voleti, Linda Petrini, Martin Weiss, Breandan Considine, Jérôme Parent-Lévesque, Kevin Xie, Kenny Erleben, et al. gradsim: Differentiable simulation for system identification and visuomotor control. In *International conference on learning representations*, 2020.
- [24] Nigamaa Nayakanti, Rami Al-Rfou, Aurick Zhou, Kratarth Goel, Khaled S Refaat, and Benjamin Sapp. Wayformer: Motion forecasting via simple & efficient attention networks. In *2023 IEEE International Conference on Robotics and Automation (ICRA)*, pages 2980–2987. IEEE, 2023.
- [25] Anton Maximilian Schaefer, Steffen Udluft, and Hans-Georg Zimmermann. A recurrent control neural network for data efficient reinforcement learning. In *2007 IEEE International Symposium on Approximate Dynamic Programming and Reinforcement Learning*, pages 151–157. IEEE, 2007.
- [26] Julian Schrittwieser, Ioannis Antonoglou, Thomas Hubert, Karen Simonyan, Laurent Sifre, Simon Schmitt, Arthur Guez, Edward Lockhart, Demis Hassabis, Thore Graepel, et al. Mastering atari, go, chess and shogi by planning with a learned model. *Nature*, 588(7839):604–609, 2020.
- [27] John Schulman, Sergey Levine, Pieter Abbeel, Michael Jordan, and Philipp Moritz. Trust region policy optimization. In *International conference on machine learning*, pages 1889–1897. PMLR, 2015.
- [28] John Schulman, Filip Wolski, Prafulla Dhariwal, Alec Radford, and Oleg Klimov. Proximal policy optimization algorithms. *arXiv preprint arXiv:1707.06347*, 2017.
- [29] Shaoshuai Shi, Li Jiang, Dengxin Dai, and Bernt Schiele. Motion transformer with global intention localization and local movement refinement. *Advances in Neural Information Processing Systems*, 35:6531–6543, 2022.
- [30] David Silver, Aja Huang, Chris J Maddison, Arthur Guez, Laurent Sifre, George Van Den Driessche, Julian Schrittwieser, Ioannis Antonoglou, Veda Panneershelvam, Marc Lanctot, et al. Mastering the game of go with deep neural networks and tree search. *nature*, 529(7587):484–489, 2016.
- [31] Ilya Sutskever, Oriol Vinyals, and Quoc V Le. Sequence to sequence learning with neural networks. *Advances in neural information processing systems*, 27, 2014.
- [32] Richard S Sutton, David McAllester, Satinder Singh, and Yishay Mansour. Policy gradient methods for reinforcement learning with function approximation. *Advances in neural information processing systems*, 12, 1999.
- [33] Hado Van Hasselt, Arthur Guez, and David Silver. Deep reinforcement learning with double q-learning. In *Proceedings of the AAAI conference on artificial intelligence*, volume 30, 2016.
- [34] Yu Wang, Tiebiao Zhao, and Fan Yi. Multiverse transformer: 1st place solution for waymo open sim agents challenge 2023. *arXiv preprint arXiv:2306.11868*, 2023.
- [35] Ziyu Wang, Tom Schaul, Matteo Hessel, Hado Hasselt, Marc Lanctot, and Nando Freitas. Dueling network architectures for deep reinforcement learning. In *International conference on machine learning*, pages 1995–2003. PMLR, 2016.
- [36] Nina Wiedemann, Valentin Wüest, Antonio Loquercio, Matthias Müller, Dario Floreano, and Davide Scaramuzza. Training efficient controllers via analytic policy gradient. In *2023 IEEE International Conference on Robotics and Automation (ICRA)*, pages 1349–1356. IEEE, 2023.
- [37] Daan Wierstra, Alexander Förster, Jan Peters, and Jürgen Schmidhuber. Recurrent policy gradients. *Logic Journal of IGPL*, 18(5):620–634, 2010.
- [38] Ye Yuan, Xinshuo Weng, Yanglan Ou, and Kris M Kitani. Agentformer: Agent-aware transformers for socio-temporal multi-agent forecasting. In *Proceedings of the IEEE/CVF International Conference on Computer Vision*, pages 9813–9823, 2021.
- [39] Tianhao Zhang, Gregory Kahn, Sergey Levine, and Pieter Abbeel. Learning deep control policies for autonomous aerial vehicles with mpc-guided policy search. In *2016 IEEE international conference on robotics and automation (ICRA)*, pages 528–535. IEEE, 2016.